GEOPHYSICAL RESEARCH LETTERS, VOL. 28, NO. 9, PAGES 1791-1794, MAY 1, 2001

New Information on the Deep Lunar Interior from an Inversion of Lunar Free Oscillation Periods

A. Khan and K. Mosegaard

Dept. of Geophysics, Niels Bohr Institute, University of Copenhagen, Denmark.

Abstract. We have obtained crucial information on the deep lunar interior through a Monte Carlo inversion of a number of fundamental lunar spheroidal free oscillations. The results indicate a homogeneous upper mantle with a velocity and density of 3.75±1.1 km/s and 3.3±0.5 g/cm^3. A transition between the upper and middle mantle in the range 520-580 km depth also seems to be implied. Middle mantle velocities and densities are 5.4±1.2 km/s and 3.5±0.2 g/cm^3. Moreover, a velocity decrease is seen in the lower mantle (1150-1450 km depth) consistent with earlier inferences of partial melt in this region. The density seems to increase gradually from 1250 km depth to the center of the moon, where it reaches values indicative of an FeS or silicate composition.

Introduction

Seismology has so far provided the most detailed information on the lunar interior of all geophysical methods used to sense its structure. However, the analysis of the seimic data, obtained from a four-station array placed on the lunar surface during the Apollo missions, was beset by numerous problems, notably the complexity of the seismic signals caused by intense scattering and the small number of usable events [*Lammlein et al.*, 1974; *Toksöz et al.*, 1974]. The analysis of these data throughout the 70ies and early 80ies led to models of the lunar interior velocity structure [*e.g. Goins et al.*, 1981; *Nakamura et al.*, 1974, 1976, 1982; *Toksöz et al.*, 1974] with details remaining perfunctory. Recently, we reanalysed the seismic data using a statistically more rigorous Monte Carlo method [*Khan et al.*, 2000], to constrain velocity variations in the mantle. However, as was the case with previous studies information was limited to a depth of roughly 1100 km, because of the distribution of the seismic sources, leaving the question concerning the structure of the lower mantle and central region unanswered. Given the ingrained complexity of the lunar seismic signals a full wave form analysis is currently not feasible, thus leaving few other alternatives. The studies mentioned above used ray theory as an approximation to the wave equation in order to invert the only unambiguously decipherable phases, namely the first P and S-wave arrivals. This obviously represents the high frequency aspect of the seismic signals. In this study, we investigate free oscillation periods corresponding to the low frequency part of the signals. An earlier attempt at identifying lunar free oscillations, using two of the events considered here, suggested that some of the Moon's spheroidal free oscillations had been observed [*Loudin*, 1979]. However, no attempt at inverting the data was made. The study was essentially limited to forward modeling, i.e. the velocity model by Nakamura was employed to predict free oscillation periods which were then matched up with the observed spectral peaks. The assumed velocity model was then modified so as to agree with as many peaks as possible and in this manner a number of structural-compositional models were analysed. A preliminary inversion conducted by us [*Khan and Mosegaard*, 2000] using exactly those periods designated by Loudin resulted in the Nakamura velocity structure, which was to be expected since, as mentioned, it was employed to predict periods of normal modes in the first place. Here, we have inverted a number of fundamental lunar spheroidal modes to obtain information on the central parts of the moon and furthermore to prevent the introduction of any subjective bias in this study, we have abstained from assigning normal modes to observed spectral peaks. Also, the periods of free oscillations of the moon are relevant to the question of a possible core, since the state of the core profoundly affects the fundamental modes of free oscillation of the moon, with the gravest spheroidal mode (${}_0S_2$) being the most sensitive.

Paper number 2000GL012445.
0094-8276/01/2000GL012445$05.00

Analysis

In the last years of the lunar passive seismic experiment the long period instruments at station 12, 15 and 16 were operated in the flat mode, i.e. instrumental response extended to low frequencies. We searched through the entire data set [*Nakamura et al.*, 1981] in this interval (1975 day 180 to 1977 day 86) and the largest events to occur in this period were a number of meteoroid impacts of which 5 were selected for analysis (impacts on day 13, 25, 121, 137 and 319 of 1976). Only the vertical components at each station have been used, however, because of non-seismic disturbances in the horizontal components of the seismometers which are believed to be caused by thermal expansions coinciding with lunar sunrise and sunset [*Latham et al.*, 1972]. This eliminates the possibility of examining toroidal modes of free oscillation, thus leaving only the spheroidal modes. Initially, impacts on day 149 and 235 had also been selected, but were discarded because in these cases even the vertical-component data were contaminated with non-seismic interference. The time series analysed were approximately 163 min long, starting about 5 min before the first P-wave arrival. Any obvious errors in the data (see *Nakamura* (1992) for details) were removed by suppressing these to the mean level of the signal. The records were subsequently zero-meaned and Hann-tapered at both ends using a 3000-sample (sampling rate 151 ms) window. Normalised amplitude spectra were then obtained using the Yule-Walker autoregressive method, which derives an all-pole model to represent the spectrum. Since we chose the number of poles to be

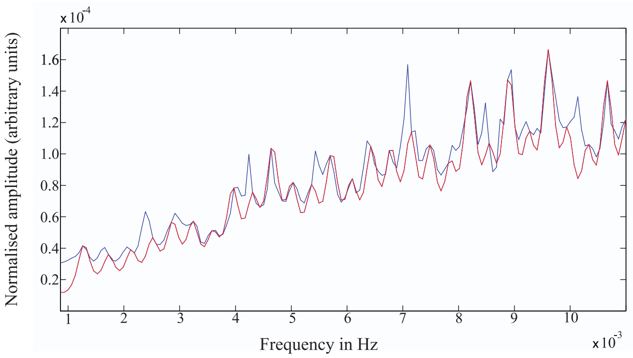

Figure 1. The stacked amplitude spectrum (blue line) and an example of a synthetic amplitude spectrum (red line), depicting a data fit. The uncertainty on an observed spectral amplitude was estimated by noting the standard deviation for that given amplitude among the individual spectra of the five meteoroid impacts prior to stacking.

1/5 the number of spectral features that we want to fit, the spectra are smoothed. All spectra were ensuingly stacked and these spectral peaks comprise the observed data, whose signal-to-noise ratio was estimated to be 1.9. As in our previous analysis [*Khan et al.*, 2000] we use an inverse Monte Carlo (MC) sampling method to solve the non-linear inverse problem, although slightly refined in that a Gibbs sampler is employed [*Gelfand and Smith*, 1990; *Geman and Geman*, 1984]. The forward routine which calculates the periods of a given set of normal modes uses as input a parametrised density, P and S-wave velocity model. This being an iterative process, oscillation periods for a given number of normal modes are being calculated for every density, P and S-wave velocity model proposed by the MC algorithm. Synthetic spectra are calculated as a superposition of spectral peaks using functions of the form $k_1/(1+k_2 \cdot f^2)$, where k_1 and k_2 are constants and f is the frequency. In the absence of information regarding the focal mechanism synthetic amplitudes of individual spectral peaks cannot be estimated. Therefore, we have chosen to fit to a given calculated frequency the most optimal amplitude, corresponding to the observed amplitude at that particular frequency. This is considered an adequate approximation to the actual synthetic spectrum (the actual synthetic spectrum is distinguished from the one we are using by also containing the corresponding proper amplitudes) for a given lunar density and velocity model in that errors in our synthetic spectrum are confined to the amplitudes of the rather narrow spectral peaks, and these errors contribute little to the calculated misfit. The amplitude of a given calculated mode is obtained by solving the following equation for the coeffecients b_j: $a_{obs}(f_i) = \sum_j b_j M_{ij}$, where $a_{obs}(f_i)$ is the observed amplitude for frequency or mode i and $M_{ij} = k_1/(1 + k_2 \cdot (f_i - f_j)^2)$, with the sum extending over all calculated modes j. This is a linear problem, which is easily solved using standard techniques and whose solution is given by $\mathbf{b} = (\mathbf{M^T M})^{-1}\mathbf{M^T a_{\mathrm{obs}}}$. The main advantage of this method is that the subjectivity in indentifying spectral peaks is bypassed, by not having to assign a certain mode to a peak beforehand, since the period of a given mode is highly dependent on the velocity model, of which we essentially assume ignorance. This leads to an overall more consistent analysis. At every step then, that the MC algorithm proposes a new density, P and S-wave velocity model, the misfit is simply given by $\|a_{obs}(f_i) - \sum_j M_{ij} y_j\|^2/\sigma_i^2$, where the y_j now represent the solutions of the above equation and σ_i is the uncertainty on the ith spectral amplitude. This means that models resulting in a good agreement between observed and calculated spectral peaks are more likely to be sampled than others. It should be added that sampled density models were at the same time made to fit the constraints of total lunar mass and moment of inertia (henceforth abbreviated M and I). As regards the errors mentioned above, their action is to bias the misfit toward smaller values, in the sense that our synthetic spectral peak amplitudes always fit the observed perfectly, whereas the actual synthetic amplitudes would either be higher, equal to or smaller than the observed ones. The sampled posterior distribution will, as a consequence, deviate from the true posterior distribution, which we would be sampling if we were able to calculate the actual synthetic spectrum, by being more broad and flat (a direct outcome of less information). Ultimately, this means a more conservative estimate of model parameter uncertainties.

The first 29 fundamental spheroidal oscillations, starting with the gravest mode $_0S_2$ and up to $_0S_{30}$ are modeled in the range 0.86 mHz - 11.0 mHz, corresponding to the observed frequency range. Fig. 1 shows the stacked spetrum as well as an example of a synthetic spectrum.

Results and Discussion

The resulting lunar S-wave velocity and density structure are depicted in fig. 2. Before delineating the results, a number of points related to the numerical modeling in this study should be asserted. First of all it is to be noted that the density structure has been regularised in such a way that models with density increases rather than decreases are favored, although the latter are not excluded by the algorithm. This is justified given that density inversions in the lunar mantle are unlikely to persist, since subsolidus convective mixing has probably been a significant process in early lunar history [*Hood and Jones*, 1987]. The inevitable assumption of radial symmetry has been invoked, implying a laterally homogeneous moon and moreover since normal modes involve movement of the whole body, the results are to be viewed as average velocities for the entire moon. The outcome, nonetheless provides independent evidence and further constraints on the interior velocity and density structure to our model obtained through arrival time inversion. Specifically, the results indicate a homogeneous upper mantle comprising a roughly constant S-wave velocity around 3.75±1.1 km/s down to a depth of about 500 km. A transition in the depth range 520-550 km between the upper and middle mantle seems furthermore to be implied by the results here. Continuing, the velocity seems to increase to about 5.4±1.2 km/s at 780 km depth. This value seems to persist throughout the middle mantle down to about 1150 km depth. These results are in rough agreement with those from our earlier study [*Khan et al.*, 2000]. From hereon the results are indicative of a decrease in S-wave velocity to 4.5±1.4 km/s in the lower mantle, comprising the depth range 1150-1450 km. The transition at 1150 km depth is taken to be the interface between the middle and lower mantle. This decrease is probably due to the presence of some partial melt. A partial melt of a few percent in the lower mantle material had been infered earlier to explain the absence of shear wave arrivals at two of the four stations from the relatively strong deep

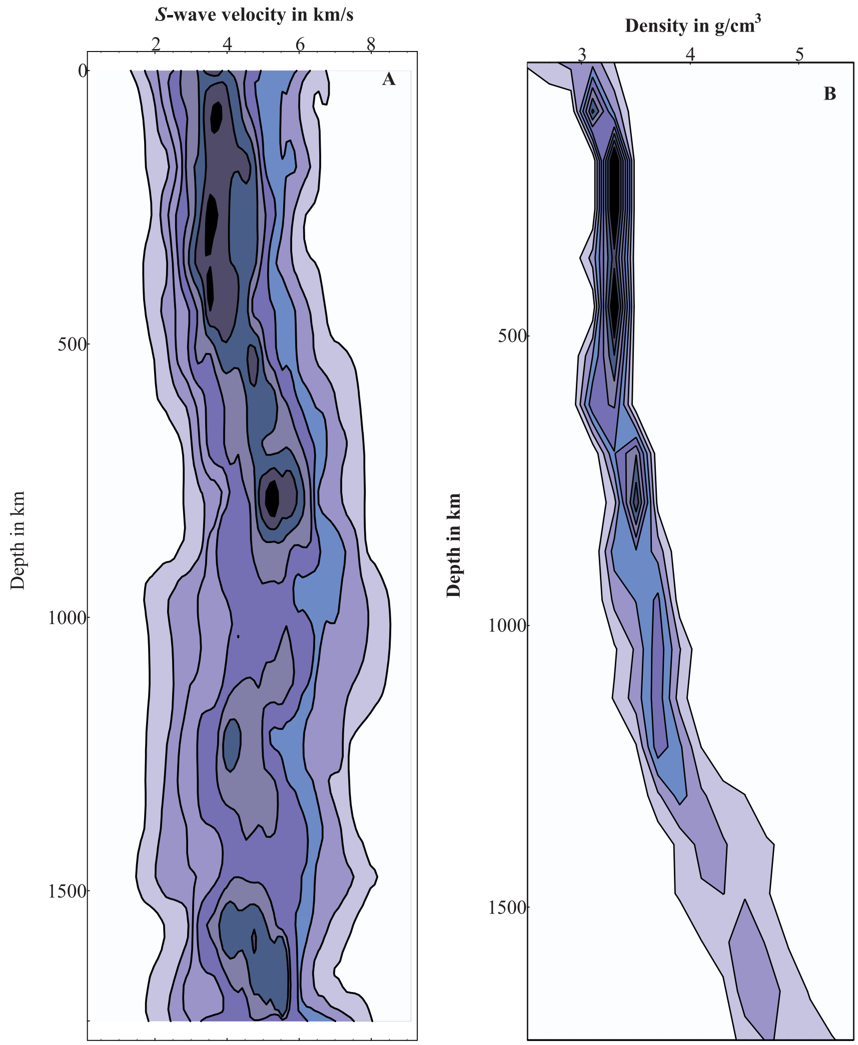

Figure 2. (A) Marginal posterior velocity distributions and (B) marginal posterior density distributions depicting the velocity and density as a function of depth. For every 100 kilometers a histogram reflecting the marginal probability distribution of sampled velocities and densities has been set up. By lining up these marginals, the velocity and density as a function of depth is envisioned as contours directly relating their probability of occurence. The contour lines define 8 equal-sized probability density intervals for the distributions. P-wave marginal posterior velocity distributions are not shown given that for spheroidal modes the compressional wave energy is confined to the upper part of the mantle, as our analysis demonstrated.

moonquake focus A_{33}, the only far-side moonquake observed which is situated just over the limb [*Nakamura et al.*, 1973]. In the central region S-wave velocities are 4.7±1.5 km/s.

Concerning the density structure variations are less apparent, although the constant homogeneous upper mantle also seems to be implied by the sampled density models. More specifically, the density appears to increase from 2.8±0.3 g/cm^3 at the surface to 3.1±0.2 g/cm^3 at the crust-mantle interface. From about 80 km and down to roughly 150 km depth, the density increases to 3.3±0.1 g/cm^3. This value seems to remain constant down to 550-580 km depth. The results indicate a further density increase to 3.5±0.2 g/cm^3 at a depth of 650 km continuing down to 850 km. In addition, the results appear to imply an further increase to 3.7±0.3 g/cm^3 in the lower part of the middle mantle at 950 km depth extending into the upper part of the lower mantle to 1250 km depth. Finally, the density in the remaining lower mantle and central region seems to increase gradually toward the center, where it assumes a value of 4.7±0.4 g/cm^3.

A few remarks concerning the derived density and velocity structures are appropriate at this point. The velocity models presented here are in rough agreement with those obtained from our arrival time inversion. The uncertainties, however, are larger directly reflecting that the particular aspect of the seismic data considered here contain less information than those considered previously. This was to be expected given that the response of the long-period instruments even while operated in the flat mode was poor for normal mode determinations. When evaluating the density structure it must be remembered that the sampled density models not only had to fit the long-period seismic data, but also the constraints of lunar mass and moment of inertia, which are very well determined, thereby obviously constraining sampled densities more than velocities. The long-period seismic data limited information on density structure down to the middle mantle, while the remaining lower mantle and central region are being constrained by M, I and the additionally introduced regularisation inclined towards increasing densities with depth. As is apparent densities appropriate for an iron core are not achieved in the central region. Densities seem to be more in the realm of an FeS or silicate core, although an Fe core cannot rigorously be excluded. The mean moment of inertia and mass density calculated using the density models from this study are 0.3931 (I/MR^2) and 3.344 g/cm^3 in agreement with the latest values obtained from Lunar Prospector [*Konopliv et al.*, 1998].

Acknowledgments. We are grateful to Guy Masters and Gabi Laske for a copy of the code comprising the forward routine. Constructive reviews by Albert Tarantola and Paul Warren are highly appreciated. We also wish to thank Yosio Nakamura for comments improving the manuscript. Finally, we would like to thank Chico Voss for his help with extracting data from the event tapes.

References

Gelfand, A. and Smith, A., Sampling Based Approaches to Calculating Marginal Densities, *J. Amer. Statist. Assoc., 85,* 398, 1990.

Geman, S. and Geman, D., Stochastic Relaxation, Gibbs Distribution and the Bayesian Restoration of Images, *I.E.E.E., Trans. Pattern Anal. Mach. Intell., 6,* 721, 1984.

Goins, N., Dainty, A. and Toksöz, M. N., Lunar Seismology: The Internal Structure of the Moon, *J. of Geophys. Res., 86*, 5061, 1981.

Hood, L. and Jones, J., Geophysical Constraints on Lunar Bulk Composition and Structure: A Reassessment, *J. Geophys. Res., 92*, E396, 1987.

Khan, A., Mosegaard, K. and Rasmussen, K. L., A New Seismic Velocity Model for the Moon from a Monte Carlo Inversion of The Apollo Lunar Seismic Data, *Geophys. Res. Lett., 27*, 1591, 2000.

Khan, A. and Mosegaard, K., Preliminary Results from a Study of the Free Oscillation Periods of the Moon, In *Lunar and Planetary Science XXXI*, abstract #1343, Lunar and Planetary Institute, Houston (CD-ROM), 2000.

Konopliv, A., Binder, A., Hood, L., Kucinskas, A., Sjogren, W. and Williams, J., Improved Gravity Field of the Moon from Lunar Prospector, *Science, 281*, 1476, 1998.

Lammlein, D., Latham, G., Dorman, J., Nakamura Y. and Ewing, M., Lunar Seismicity, Structure and Tectonics, *Rev. Geophys. Space Phys., 14*, 224, 1974.

Latham, G. V., Ewing, M., Press, F., Sutton, G., Dorman, J., Nakamura, Y., Toksoz, M. N., Lammlein D. and Duennebier, F., Passive Seismic Experiment, in *Apollo 16 Preliminary Science Report, NASA SP-315*, Sec. 9, 29pp., 1972.

Loudin, M., Structural-Compositional Model of the Lunar Interior, M. S. Thesis, Pennsylvania State University, University Park, 1979.

Nakamura, Y., Lammlein, D., Latham, G., Ewing, M., Dorman, J., Press, F., and Toksöz, N., New Seismic Data on the State of the Deep Lunar Interior, *Science, 181*, 49, 1973.

Nakamura, Y., Latham, G., Dorman, J. and Harris, J., Passive Seismic Experiment Long-Period Event Catalog, Final Version, 1969 day 202 - 1977 day 273, 314 pp., Galveston Geophysics Laboratory Contribution No. 491, University of Texas at Austin, 1981.

Nakamura, Y., Latham, G. and Dorman, J., Apollo Lunar Seismic Experiment- Final Summary, *J. Geophys. Res., 87*, A117, 1982.

Nakamura, Y., Catalog of Lunar Seismic Data from Apollo Passive Seismic Experiment on 8-mm Exabyte Tapes, p.7-9, UTIG Technical Report No. 118, University of Texax at Austin, 1992.

Toksöz, M. N., Dainty, A., Solomon, S. C. and Anderson, K., Structure of the Moon, *Reviews of Geophysics and Space Physics, 12*, 539, 1974.

A. Khan and K. Mosegaard, Department of Geophysics, Niels Bohr Institute for Astronomy, Physics and Geophysics, University of Copenhagen, Juliane Maries Vej 30, 2100 Copenhagen O, Denmark. (e-mail: amir@gfy.ku.dk; klaus@gfy.ku.dk)

(Received October 4, 2000; revised February 5, 2001; accepted February 9, 2001.)